Journal of Catalysis 271 (2010) 386–391

Contents lists available at ScienceDirect

Journal of Catalysis

journal homepage: www.elsevier.com/locate/jcat

Catalytic activity and selectivity of methylbenzenes in HSAPO-34 catalyst for the methanol-to-olefins conversion from first principles

Chuan-Ming Wang [a,b], Yang-Dong Wang [a], Hong-Xing Liu [a], Zai-Ku Xie [a,*], Zhi-Pan Liu [b,**]

[a] Shanghai Research Institute of Petrochemical Technology, SINOPEC, Shanghai 201208, China
[b] Shanghai Key Laboratory of Molecular Catalysis and Innovative Materials, Department of Chemistry, Fudan University, Shanghai 200433, China

ARTICLE INFO

Article history:
Received 7 December 2009
Revised 1 February 2010
Accepted 22 February 2010
Available online 8 April 2010

Keywords:
Methanol-to-olefins conversion
HSAPO-34 catalyst
Methylbenzenes
Zeolite
Density functional theory calculations

ABSTRACT

As an attractive alternative to produce light olefins, methanol-to-olefins (MTO) conversion catalyzed by zeolites or zeotype materials was recently proposed to follow a hydrocarbon pool mechanism. In this contribution, the effect of the structure of methylbenzenes (MBs) in the pore of HSAPO-34 catalyst on the MTO activity and selectivity is investigated by first-principle calculations and kinetic simulations. We demonstrate that MBs with five or six methyl groups are not more active than those with fewer methyl groups. Propene is intrinsically more favorable than ethene when the reaction is not diffusion limited based on the side-chain hydrocarbon pool mechanism. Our theoretical results are consistent with some experimental observations and can be rationalized based on the shape selectivity of key reaction intermediates and transition states in the pore of catalyst.

1. Introduction

The conversion of MTO over zeolites or zeotype materials such as HZSM-5 and HSAPO-34 provides an attractive alternative to produce light olefins without the involvement of fossil oil [1]. Both experimental and theoretical studies have been conducted to understand the key step in the process, namely the formation of the first carbon–carbon bond from methanol [2–20]. Recently, a reaction scheme known as the hydrocarbon pool mechanism was proposed. In the mechanism, certain organic reaction centers trapped in the pore of catalysts such as MBs serve as scaffolds/cocatalysts, where methanol is added and olefins are eliminated in a closed catalytic cycle [2–4]. It is therefore indicated that the interplay between the inorganic framework and the organic reaction centers dictates the activity and selectivity. As for the evolution of hydrocarbon pool species in the MTO reaction, two possible routes, namely the side-chain route and the paring route, have been suggested. The side-chain route involves the stepwise growth of alkyl side chain on MBs and the subsequent elimination of the side chain into light olefins, while in the paring route, olefins are yielded via the contraction of MB ring [4].

To date, it remains to be a significant challenge to unravel the structure–activity relationship in the MTO reaction not least because of the complexities of the catalyst structure and the reaction network [7,21–25]. Song et al. in their early experiment suggested that both the MTO activity and propene selectivity increases with the average number of methyl groups per benzene ring catalyzed by MBs in HSAPO-34 catalyst [7]. This was supported by their thermodynamics calculation on the elimination of side alkyl chains based on 8T (octatetrahedral) cluster model of HZSM-5 [18]. More recently, Lesthaeghe et al. investigated some crucial reaction steps of side-chain route using both small and large zeolite cluster models of HZSM-5 [25]. They suggest that ethene cannot be eliminated from the side chain. One of the key issues in the field is therefore to pinpoint how the structure of MBs inside the pore of catalysts affects the activity and selectivity of the MTO reaction from the atomic level.

Here, we utilize first-principle calculations together with kinetic Monte Carlo simulations to elucidate the activity and selectivity of MBs (the number of side methyl groups is from 2 to 6) in HSAPO-34 catalyst. By exploring the energy variations of the key elementary steps with respect to the number and the position of methyl groups, we reveal that MBs with five or six methyl groups are not more active than those with four or fewer methyl groups. Propene is always the preferred product when the reaction is not diffusion limited. Importantly, we demonstrate from the atomic level how the kinetics of key elementary steps is affected by the pore topology of zeotype catalyst, which is of general importance in zeolite catalysis [18–20,26–28].

* Corresponding author. Fax: +86 21 68461279.
** Corresponding author. Fax: +86 21 65642400.
E-mail addresses: xzk@sinopec.com (Z.-K. Xie), zpliu@fudan.edu.cn (Z.-P. Liu).

0021-9517/$ - see front matter © 2010 Elsevier Inc. All rights reserved.
doi:10.1016/j.jcat.2010.02.025

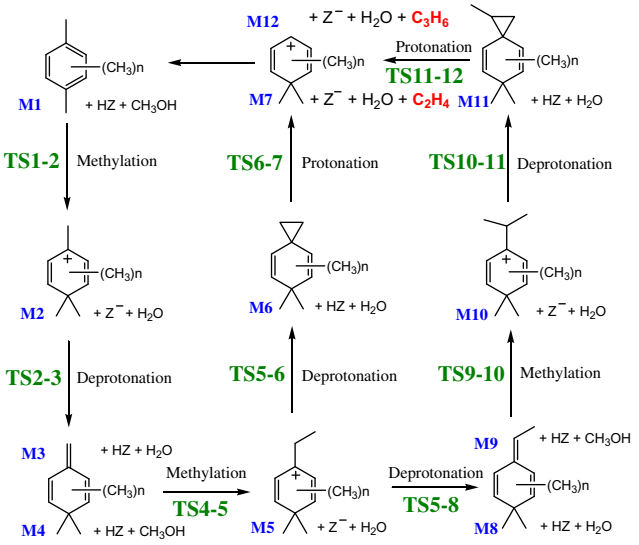

Scheme 1. Side-chain hydrocarbon pool mechanism for the MTO reaction catalyzed by MBs in acid zeotype catalyst (HZ).

2. Computational methods and modeling

All density functional theory (DFT) calculations were performed using DMol^3 package with all-electron double-numerical basis sets with polarization functions (DNP) [29–31]. The exchange-correlation functional utilized was at the generalized gradient approximation (GGA) level known as Perdew–Burke–Ernzerhof (PBE) functional. The real space cutoff distance was 5.0 Å. The reciprocal space integration over Brillouin zone was approximated by summing over a finite set of k-points with a grid separation of 0.05 Å^{-1} according to the Monkhorst–Pack scheme [32]. The eigenvector following method based on vibrational analysis was employed to search for the transition state [33]. The Bortz–Kalos–Lebowitz (BKL) kinetic Monte Carlo algorithm was used to calculate the turnover frequencies (TOFs) at 700 K [34]. The DFT-D method was employed to correct the energy of a system by taking the dispersion effects into account [35,36].

The unit cell of HSAPO-34 zeotype catalyst ($a = b = c = 9.421$ Å, $\alpha = \beta = \gamma = 94.2°$) is derived from CHA structure (all Si atoms are equivalent by symmetry), in which all Si atoms are first substituted by P and Al atoms alternatively, and one P atom then is replaced by a Si atom to generate one Brønsted acid site per cage. In our simulation of reactions, all atoms in the cell are allowed to relax with the lattice constants being fixed.

3. Results and discussion

Our exploration of the reaction paths is based on the side-chain hydrocarbon pool mechanism, which is summarized in Scheme 1. The whole catalytic cycle is initiated by the gem-methylation of MBs to form methylbenzenium cations (M1 → M2, the first methylation step). This is then followed by the growth of the side chain via repeated deprotonation of benzenium cations (M2/M5 → M3/M8 for ethene/propene paths, respectively) and methylation of exocyclic double bond intermediates (M4/M9 → M5/M10, the second and third methylation steps). Ethene/propene can finally be released from the side ethyl/isopropyl groups of benzenium cations by the elimination steps via deprotonation (M5/M10 → M6/M11) and subsequent protonation (M6/M11 → M7/M12) steps. The intermediates M6 and M11 feature spiro structure at the side chain. It was shown from theory that water should directly be involved in the reaction to facilitate the frequent proton shift between inorganic framework and organic intermediates [37].

Six different MBs have been considered in this study, including p-xylene (PX), 1,2,4-trimethylbenzene (TriMB), 1,2,3,5-tetramethylbenzene (TMB), 1,2,4,5-tetramethylbenzene, pentamethylbenzene (PMB), and hexamethylbenzene (HMB). As illustrated in Fig. 1, all these MBs can fit inside the cage of HSAPO-34 catalyst with the optimized ring structure being plane-like. HSAPO-34 has a chabazite-based (CHA) structure with large cavities (9.4 Å in diameter) connected by small eight-ring pore openings (3.8 × 3.8 Å) and is currently the preferred catalyst for the MTO reaction [38]. Nine different pathways have been investigated, which can be distinguished by the structures of benzenium cations involved, as shown in Fig. 1. For the initial stage of the reaction where methanol adsorbs at the acid site of HSAPO-34 (M1), the calculated adsorption energies of methanol range from 0.87 to 0.93 eV, which are little affected by the presence of MBs in the catalyst. The M1 state is thus a good reference state for the comparison of activity among different pathways.

The reaction profiles for nine pathways were then determined and that for the PX pathway as a representative was shown in Fig. 2 (the others were shown in Supplementary material). In general, the most stable intermediate species in the reaction pathway are benzenium cations. Compared to the M1, the first methylation products, the benzenium cations (M2) are generally less stable. The benzenium cations (M5, M10) produced from the second and third methylation are more stable than M2 due to the charge donation effect of the growing side chain. The least stable species feature either an exocyclic double bond (M3, M4, M8, M9) or a spiro structure (M6, M11), which are formed by the deprotonation of benzenium cations. The relative stability of intermediates with side ethyl or isopropyl groups and with exocyclic double bond is consistent

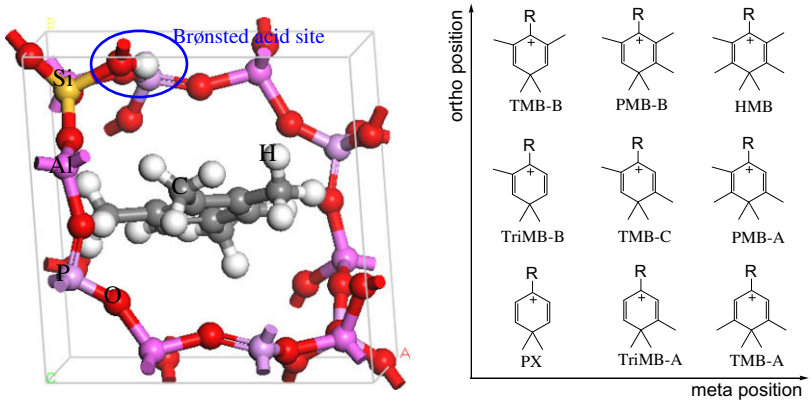

Fig. 1. Optimized structure of 1,2,3,5-tetramethylbenzene in HSAPO-34 catalyst (left) and the represented methylbenzenium cations in each pathway (right). R can be methyl (M2), ethyl (M5), or isopropyl (M10) groups.

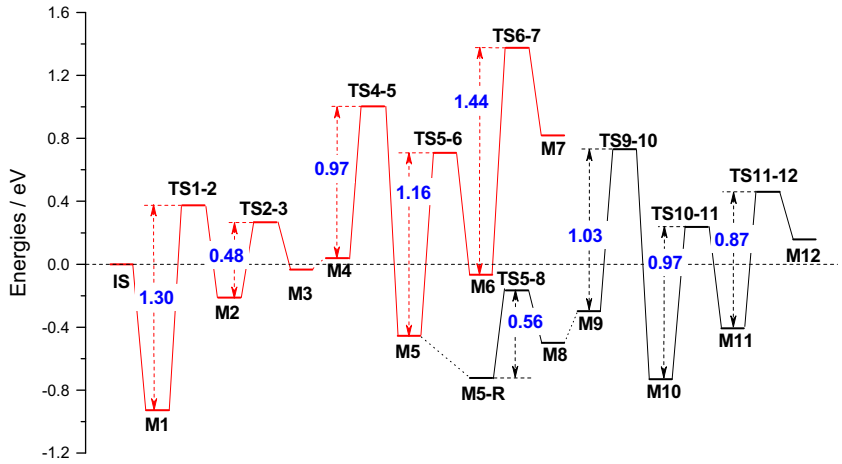

Fig. 2. Energy profile of the pathway PX in the side-chain hydrocarbon pool mechanism on HSAPO-34 catalyst. All energies are referenced to the energy of PX/HSAPO-34 and three methanol molecules in the gas phase (IS).

with those calculated in the gas phase [18]. In the following, we will elaborate on the kinetics of the pathways with special emphasis on the effect of the structure of MBs on the MTO activity and selectivity.

P-xylene (PX) is the smallest MB which can act as the reaction center for the MTO reaction according to the side-chain mechanism. As shown in Fig. 2, the reaction barriers are 1.30, 0.97, and 1.03 eV for the first, the second, and the third methylation step, respectively. Our results from periodic DFT calculations are similar to those calculated using MFI structure by ONIOM model (1.37 and 1.03 eV for the first and the second methylation steps, in which exocyclic double bond is located in the ortho position relative to the gem-methylated site) [25,27]. The formation of the exocyclic double bond by deprotonation is generally facile with the reaction barriers of about 0.50 eV due to the promotion effect of water [37]. The elimination steps to form propene and ethene are endothermic by 0.92 and 1.28 eV, respectively, and thus are difficult kinetically. The values are in the same trend with those calculated using 8T cluster model of HZSM-5 (0.98 and 1.14 eV for propene and ethene) [18]. The barrier to propene (1.19 eV, M10 → M12) is much lower than that to ethene (1.83 eV, M5 → M7). According to the PX pathway, it can be seen that the slow reaction steps include three methylation steps and two final elimination steps, as shown in Table 1, where the calculated values for all the other pathways are also listed for comparison. The reaction barriers corrected by the DFT-D method to include the dispersion energy are shown in the Supplementary material, Table S1. We found that the inclusion of dispersion interactions slightly decreases the reaction barriers in the methylation and deprotonation steps while increases those in the elimination steps systematically. The trend for the catalytic activity of different MBs as concerned in this work is not affected by the dispersion energy.

It should be mentioned that the first methanol molecule adsorbs at the image acid site in our model [37]. The reason that we adopt this model is to avoid the rotation of bulky cyclic intermediates inside the cage of HSAPO-34 catalyst. On the other hand, our model is compatible with the real situation since the concentration of acid sites is as high as three per cage in some HSAPO-34 samples, and the structure of AlPO-34 (the prototype of HSAPO-34 model) is highly symmetrical [17]. Nevertheless, we also checked the reaction barrier in the first methylation step of PX when methanol is at the acid site, which is calculated to be 1.27 eV, in consistent with 1.30 eV when methanol is at the image position. This indicates that the methylation barrier is less affected by the position of the acid site where methanol adsorbs.

With reference to the PX pathway, it is possible to reveal the effect of additional methyl groups on the reaction barrier of the elementary step. First, we found that the methyl groups meta to the departing alkyl (ethyl or isopropyl) group can lower the reaction barriers of the first methylation step (M1 → M2: PX > TriMB-A > TMB-A, TriMB-B > TMB-C > PMB-A, and TMB-B > PMB-B > HMB) by about 0.20 eV. By contrast, the deprotonation steps to form exocyclic double bond (M2 → M3, M5 → M8) become more difficult with meta methyl groups as the barriers increase up to 0.40 eV for M2 → M3 and 0.80 eV for M5 → M8. These can be attributed to the enhanced stability of benzenium cations (M2, M5) in the presence of additional meta methyl groups, considering that methyl groups can help stabilize the cation via the resonance structures. Very recently, the deprotonation barriers (M2 → M3) were calculated using a 5T cluster model [25]. It was found that

Table 1
Reaction barriers of identified key steps in the side-chain hydrocarbon pool mechanism for the MTO reaction catalyzed by MBs in HSAPO-34 catalyst. The unit is eV.

	M1 → M2	M2 → M3	M4 → M5	M5 → M6	M6 → M7	M5 → M7	M5 → M8	M9 → M10	M10 → M11	M11 → M12	M10 → M12
PX	1.30	0.48	0.97	1.16	1.44	1.83	0.56	1.03	0.97	0.87	1.19
TriMB-A	1.22	0.74	1.21	1.22	1.37	1.88	0.86	1.17	1.25	0.79	1.40
TriMB-B	1.45	0.38	0.92	1.26	1.27	1.94	0.27	0.96	1.29	0.84	1.53
TMB-A	1.10	0.83	1.26	1.36	1.48	2.17	1.36	1.20	1.39	0.83	1.61
TMB-B	1.35	0.46	0.91	1.29	1.16	1.86	0.50	0.92	1.27	0.85	1.51
TMB-C	1.29	0.71	1.09	1.44	1.16	2.06	0.81	1.07	1.43	0.79	1.61
PMB-A	1.24	0.78	0.99	1.59	1.24	2.31	0.95	1.02	1.61	0.85	1.87
PMB-B	1.24	0.68	1.01	1.57	1.18	2.20	1.14	0.89	1.32	0.67	1.32
HMB [37]	1.17	0.79	0.92	1.67	1.23	2.40	1.28	0.93	1.50	0.68	1.60

the deprotonation barriers increase with the number of methyl groups on the ring, which are however much lower than our calculated results (e.g. ~0.30 and 0.79 eV in HMB pathway for cluster model and our periodic model, respectively). It is expected that this is mainly due to the absence of electrostatic stabilization of the cations in the 5T cluster model [25].

Second, the methyl groups at the ortho position can affect strongly the reaction barriers in the second and third methylation steps. A systematic decrease in the reaction barriers of M4 → M5 and M9 → M10 could be identified with the increase of ortho methyl groups (PX > TriMB-B > TMB-B, TriMB-A > TMB-C > PMB-B, and TMB-A > PMB-A > HMB). The magnitude is up to 0.34 eV for the second methylation step and 0.27 eV for the third methylation step (we will show later that the effects of the ortho methyl groups are in fact related to the pore geometry of HSAPO-34). In this case, the meta methyl groups have a role to further tune the impact of the ortho methyl groups: the more the meta methyl groups, the larger the effect of the ortho methyl groups is. For example, the magnitudes of the barrier reduction in the second methylation step are 0.06, 0.20, and 0.34 eV corresponding to zero, one, and two meta methyl groups, respectively.

Finally, we examined the effect of the methyl groups on the elimination steps (M5/M10 → M7/M12). Regarding the deprotonation steps for the formation of intermediates with spiro structure (M5/M10 → M6/M11), the reaction barriers increase with the addition of meta methyl groups, and this trend is similar to the effect observed above for the formation of exocyclic double bond intermediates. The barriers of the subsequent protonation step (M6 → M7 and M11 → M12) are less sensitive to the additional methyl groups. Overall, it can be seen that the elimination barriers of ethene (M5 → M7) and propene (M10 → M12) from side ethyl and isopropyl chains increase upon the addition of meta methyl groups (see Table 1). More importantly, the elimination barriers of ethene are generally larger than those of propene in all pathways. This can be attributed to the stability of the transition state structure (TS6-7 and TS11-12), where a hydrocarbon cation is formed at the β-C of the side chain through the protonation step. In the propene formation, the β-C cation is a secondary carbon, while it is a primary carbon in the ethene formation.

It is noted that several alternative routes for the elimination of side alkyl chains from ethylbenzene (or ethylbenzenium) and propylbenzene (or propylbenzenium) in zeolites have also been investigated [39–42]. A concerted route for the dealkylation of ethylbenzene and isopropylbenzene was identified theoretically using 4T cluster model, and the calculated reaction barriers are quite high [39,40]. It was shown that the elimination of isopropyl group is easier than that of ethyl group. Other intramolecular hydride shift route has also been proposed [41,42]. Our previous work has shown that the intermolecular proton shift route is more favorable than intramolecular hydride shift route in the elimination of side chains, and the intermediates featuring spiro structure are relatively unstable [37]. This was confirmed by recent theoretical studies on HZSM-5 model [25].

For a complex reaction network involving multiple elementary steps, a kinetic simulation is essential to determine the activity and selectivity. In this work, we have utilized the kinetic Monte Carlo algorithm to simulate the overall rate of the nine different pathways. From the kinetic simulation, we found that (i) on all the systems investigated, propene is always preferentially produced than ethene when the reaction is not diffusion limited, which is consistent with the energetic feature seen from the reaction energy profiles and (ii) the rate-determining step for the elimination of propene is the methylation of exocyclic double bond (M9 → M10 in HMB pathway and M4 → M5 in the other pathways) [37], while that for the production of ethene is the elimination step from the spiro intermediate (see Table 2).

Table 2
The overall barriers of the production of ethene and propene catalyzed by MBs in HSAPO-34 catalyst by different models. The unit is eV.

	Ethene ($1 \times 1 \times 1$ model)	Propene ($1 \times 1 \times 1$ model)	Propene ($1 \times 2 \times 1$ model)
PX	2.30 (M1 → TS6-7)	1.93 (M1 → TS4-5)	1.84
TriMB-A	2.32 (M1 → TS6-7)	2.14 (M1 → TS4-5)	2.11
TriMB-B	2.32 (M1 → TS6-7)	1.94 (M1 → TS4-5)	1.94
TMB-A	2.41 (M1 → TS6-7)	2.09 (M1 → TS4-5)	2.06
TMB-B	2.18 (M1 → TS6-7)	1.86 (M1 → TS4-5)	1.88
TMB-C	2.41 (M1 → TS6-7)	2.10 (M1 → TS4-5)	2.09
PMB-A	2.57 (M1 → TS6-7)	2.18 (M1 → TS4-5)	2.09
PMB-B	2.51 (M1 → TS6-7)	2.06 (M1 → TS4-5)	2.10
HMB [37]	2.59 (M1 → TS6-7)	2.14 (M1 → TS9-10)	1.96

In Fig. 3, we have plotted the calculated TOFs at 700 K against the apparent barriers for propene production, which are the overall barrier height from M1 to M5 or M10 obtained readily from potential energy profile plot (such as Fig. 2). The linear relationship as shown in Fig. 3 confirms that although the reaction network appears quite complex, the rate for propene formation is directly related to the highest energy transition state involved in the pathway. The results show that 1,2,3,5-TMB and PX are the most active species for the MTO reaction, while PMB and HMB are not more active than MBs with fewer methyl groups. This is in contradiction to the earlier suggestion that HMB exhibits the highest catalytic activity [7]. Comparing the isomeric pathways, the one with more ortho methyl groups (isomers named with 'B' in Fig. 1) is generally preferred.

In order to check whether the size of unit cell will affect the activity, we also calculated the overall barriers using a larger supercell ($1 \times 2 \times 1$) of HSAPO-34 model. The results are also listed in Table 2. It can be seen that in the larger cell the PMB and HMB remain to be not more active than the other MBs with fewer methyl groups.

We are now in the position to ask why MBs with five or six methyl groups are not more active in producing propene. Is this related to the pore geometry of HSAPO-34 catalyst? According to the kinetic simulation, the overall barrier can be considered as a sum of two parts: an endothermic part from M1 to M4 or M9, and a kinetic-controlled part from the second or third methylation step. Since the concentration of M4 or M9 should be much lower than that of M1, the reaction rate of the first methylation step is thus larger than that of the second or third methylation step. The

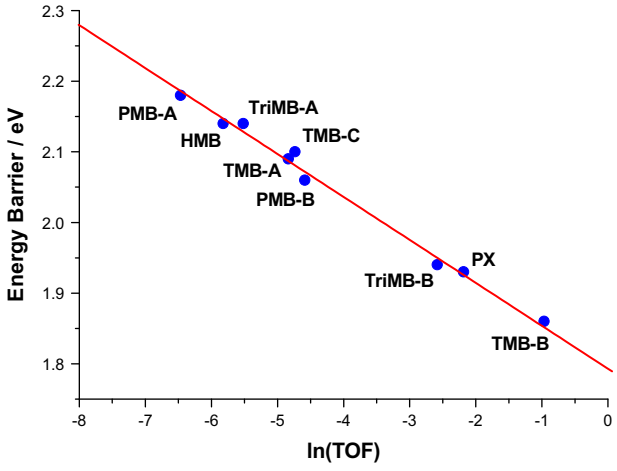

Fig. 3. The relationship between the overall barriers to propene production and the calculated TOFs at 700 K over MBs in HSAPO-34 catalyst.

Table 3
The stability of polymethylmethylene-1,4-cyclohexadiene (PMMC) in gas phase (the reaction energies from MBs and $CH_3OH_2^+$) and in the pore of HSAPO-34 catalyst (the reaction energies of M4 with reference to M1). The unit is eV.

	Gas phase	HSAPO-34	ΔE
PX	1.46	0.97	−0.49
TriMB-A	1.40	0.93	−0.47
TriMB-B	1.37	1.02	−0.35
TMB-A	1.46	0.83	−0.63
TMB-B	1.39	0.95	−0.44
TMB-C	1.39	1.01	−0.38
PMB-A	1.42	1.20	−0.22
PMB-B	1.38	1.05	−0.33
HMB [37]	1.35	1.12	−0.23

Notes. The spatial constraints of HSAPO-34 catalyst for the intermediates with exocyclic double bond can be indicated by the difference of reaction energies (ΔE) between in gas phase and in the pore of HSAPO-34 catalyst.

yield of propene can apparently be enhanced by stabilizing either the exocyclic double bond to increase the amount of M4 or M9 or stabilizing the transition state in the methylation step. We found that the stability of both structures is in fact subject to the spatial constraint imposed by the framework of catalyst.

Table 3 shows that the stability of the gas-phase intermediates with the exocyclic double bond is quite insensitive to the number and the position of side methyl groups. However, these intermediates (especially M4) inside the pore become obviously less stable (the endothermicity is over 1.05 eV) if more than four methyl groups are present, as in PMB-A, PMB-B, and HMB pathways (see Table 3). Reversely, in the other pathways with four or fewer methyl groups on the benzene ring, the steric repulsion between methyl groups and inorganic framework is much relieved and the intermediates become relatively more stable. From our results, the magnitude of the destabilization due to the methyl groups is around 0.16–0.27 eV, where the largest effect occurs, not surprisingly, in the pathway of PMB and HMB.

On the other hand, the presence of ortho methyl groups contributes to stabilize the transition state (TS4-5) in the rate-determining methylation step. To illustrate this, we may further compare the structures of TS4-5 in the isomeric pathways TMB-A and TMB-B, which are two extreme situations as the second methylation barriers of the other pathways lie in between the barriers of these two. As shown in Fig. 4a for TMB-A, the lack of sufficient space around the exocyclic double bond during the methylation step enforces the benzene ring to bend at the transition state, and the reaction barrier is as high as 1.26 eV. In TMB-B (Fig. 4b), by contrast, the planarity of the ring can well be conserved during the methylation step with the reaction barrier being only 0.91 eV. Therefore, it can be summarized that the transition state shape dictates the overall positive role of ortho methyl groups to the activity, which is a kinetic effect, while the poorest catalytic activities of

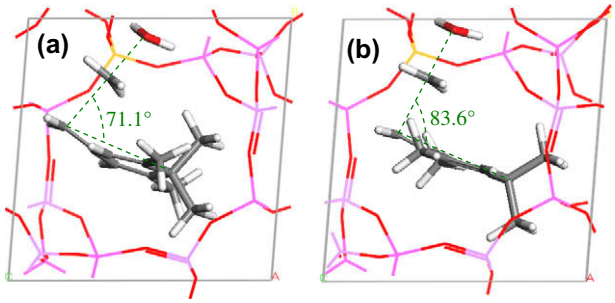

Fig. 4. Located structures for transition state TS4-5 in TMB-A (a) and TMB-B (b) pathways.

PMB and HMB can be attributed to the thermodynamic reason as mentioned previously, where the reaction intermediate shape is not compatible to the pore geometry of HSAPO-34. By identifying the key structures that are important to the overall rate, we therefore demonstrate that the interplay between the organic reaction center and the pore of catalyst plays an important role in the MTO reaction.

It might be mentioned that our results on the catalytic activity of MBs in zeotype catalyst are indirectly supported by the experimental observations. By using GC–MS to detect the reaction intermediates [10], Sassi et al. identified various forms of isopropylmethylbenzenes, which is presumably formed via demethylation from isopropylbenzenium cations: the isopropylmethylbenzenes with two and three methyl groups have the highest concentrations, while the amounts of MBs with three to six methyl groups are comparable within zeolite. Since these isopropylmethylbenzenes are formed from trimethylbenzene and tetramethylbenzene according to Scheme 1, the experimental results thus implied that MBs containing three or four methyl groups possess the highest activity, which supports our calculated results.

Experimentally, HMB was suggested to be the active species in the MTO reaction by isotopic labeling studies [5–7]. However, only negligible amounts of HMB have been detected in HSAPO-34 catalyst, while TMB and lighter MBs are the main constituent of MBs in active HSAPO-34 catalyst [17,43]. Our calculations found that the interconversion (steps of inter- and intra-shift of methyl group) of MBs is kinetically possible at reaction conditions. The amounts of MBs are thus expected to change with time dynamically on stream in the presence of methanol and olefins [17,43]. From our results based on the side-chain route, the high concentration of TMB and lighter MBs may well be the consequence that MBs with four or fewer methyl groups are responsible mainly for propene formation.

Our periodic DFT results show that in the TMB/HSAPO-34 model, the overall barriers for the production of propene and ethene by the side-chain route are 1.86 and 2.18 eV, respectively. We also noticed that in the TMB/HZSM-5 model, the overall barrier for the formation of isobutene by paring route was reported to be 2.68 eV at the ONIOM level [20]. Although a direct comparison between the two models is not likely because different theoretical approach and different olefins are involved, it does indicate that the side-chain route may be preferred compared to the paring route in the MTO reaction.

It should be mentioned that the distribution of products in the MTO reaction is affected not only by the intrinsic catalytic activity of active sites but also by the diffusion of olefins in the pore of catalyst. A full catalytic cycle of the side-chain hydrocarbon pool mechanism mainly comprises two parts: the formation of side ethyl or isopropyl chains and the elimination of such chains into light olefins. (This is also true for the paring route.) The formation of side chains is achieved by the methylation of the intermediates with exocyclic double bond, which are quite unstable compared to the initial adsorbed states. From this sense, the catalytic role of MBs as the hydrocarbon pool species is to provide an exocyclic double bond for the propagation of side chains. Since light olefins such as ethene and propene can readily be methylated by methanol [44–47], the hydrocarbon pool species in the MTO reaction may not be limited to MBs and may involve other simple olefins [9]. Therefore, to only focus on the MBs as the hydrocarbon pool species may lead to a biased understanding on the MTO reaction.

More recently, Svelle et al. introduced a dual cycle concept for the MTO conversion, in which ethene is exclusively formed from the lower MBs and propene and higher alkenes are preferentially formed from alkene methylation and interconversions [14–16]. These works have drawn the attention away from the MBs. In fact,

here we show that ethene may not be produced solely by means of the side-chain hydrocarbon pool mechanism based on MBs as the organic reaction centers.

The hydrocarbon pool mechanism using simple olefins as the organic reaction centers may be operative for the MTO reaction, and the process is self-catalytic. Our preliminary calculation results show that certain olefins, especially branched olefins, can be methylated more easily than MBs intermediates with exocyclic double bond. The subsequent cracking of the carbenium cations to produce ethene and propene is likely to be present in parallel with the side-chain route in MBs/HSAPO-34 system. A comprehensive survey on the methylation pathways of simple olefins and subsequent cracking of carbenium cations inside HSAPO-34 catalyst is under progress.

4. Conclusions

To recap, the catalytic activity and selectivity of MBs in HSAPO-34 catalyst for the MTO reaction has been addressed from theoretical calculations. We demonstrate that PMB and HMB are not more active than the other MBs with four or fewer methyl groups. Propene is the favored product via the side-chain hydrocarbon pool mechanism. The current periodic DFT results cast doubts on the earlier suggestions that MBs with fewer methyl groups are less active and tend to selectively produce ethene. We demonstrate that the kinetics of the zeolite catalysis is strongly affected by both the topology of the inorganic framework and the geometry of the organic reaction center. The interplay of them accounts for the stabilities of key reaction intermediates and transition states, which reflects the shape selectivity in zeolite catalysis. Based on our results on the selectivity of ethene and propene, we propose that the reaction channels involving organic hydrocarbon pool species other than MBs such as simple olefins may well be present in parallel with the MBs channels. The picture at the atomic level can help to establish a complete view on the complex reactions like the MTO conversion and, maybe more importantly, provides general insights into zeolite catalysis.

Acknowledgments

This work is supported by National Basic Research Program of China (2009CB623504), National Science Foundation of China (20773026, 20721063), and China Postdoctoral Science Foundation (20080440568).

Appendix A. Supplementary material

Supplementary data associated with this article can be found, in the online version, at doi:10.1016/j.jcat.2010.02.025.

References

[1] M. Stocker, Micropor. Mesopor. Mater. 29 (1999) 3.
[2] J.F. Haw, W.G. Song, D.M. Marcus, J.B. Nicholas, Acc. Chem. Res. 36 (2003) 317.
[3] J.F. Haw, D.M. Marcus, Top. Catal. 34 (2005) 41.
[4] U. Olsbye, M. Bjorgen, S. Svelle, K.P. Lillerud, S. Kolboe, Catal. Today 106 (2005) 108.
[5] W.G. Song, J.F. Haw, J.B. Nicholas, C.S. Heneghan, J. Am. Chem. Soc. 122 (2000) 10726.
[6] B. Arstad, S. Kolboe, J. Am. Chem. Soc. 123 (2001) 8137.
[7] W.G. Song, H. Fu, J.F. Haw, J. Am. Chem. Soc. 123 (2001) 4749.
[8] W.G. Song, D.M. Marcus, H. Fu, J.O. Ehresmann, J.F. Haw, J. Am. Chem. Soc. 124 (2002) 3844.
[9] A. Sassi, M.A. Wildman, J.F. Haw, J. Phys. Chem. B 106 (2002) 8768.
[10] A. Sassi, M.A. Wildman, H.J. Ahn, P. Prasad, J.B. Nicholas, J.F. Haw, J. Phys. Chem. B 106 (2002) 2294.
[11] M. Bjorgen, U. Olsbye, D. Petersen, S. Kolboe, J. Catal. 221 (2004) 1.
[12] D.M. Marcus, K.A. McLachlan, M.A. Wildman, J.O. Ehresmann, P.W. Kletnieks, J.F. Haw, Angew. Chem. Int. Ed. 45 (2006) 3133.
[13] Z.M. Cui, Q. Liu, W.G. Song, L.J. Wan, Angew. Chem. Int. Ed. 45 (2006) 6512.
[14] S. Svelle, F. Joensen, J. Nerlov, U. Olsbye, K.P. Lillerud, S. Kolboe, M. Bjorgen, J. Am. Chem. Soc. 128 (2006) 14770.
[15] S. Svelle, U. Olsbye, F. Joensen, M. Bjorgen, J. Phys. Chem. C 111 (2007) 17981.
[16] M. Bjorgen, S. Svelle, F. Joensen, J. Nerlov, S. Kolboe, F. Bonino, L. Palumbo, S. Bordiga, U. Olsbye, J. Catal. 249 (2007) 195.
[17] B.P.C. Hereijgers, F. Bleken, M.H. Nilsen, S. Svelle, K.P. Lillerud, M. Bjorgen, B.M. Weckhuysen, U. Olsbye, J. Catal. 264 (2009) 77.
[18] B. Arstad, J.B. Nicholas, J.F. Haw, J. Am. Chem. Soc. 126 (2004) 2991.
[19] D. Lesthaeghe, V. Van Speybroeck, G.B. Marin, M. Waroquier, Angew. Chem. Int. Ed. 45 (2006) 1714.
[20] D.M. McCann, D. Lesthaeghe, P.W. Kletnieks, D.R. Guenther, M.J. Hayman, V. Van Speybroeck, M. Waroquier, J.F. Haw, Angew. Chem. Int. Ed. 47 (2008) 5179.
[21] W.G. Song, J.B. Nicholas, J.F. Haw, J. Am. Chem. Soc. 123 (2001) 121.
[22] L. Palumbo, F. Bonino, P. Beato, M. Bjorgen, A. Zecchina, S. Bordiga, J. Phys. Chem. C 112 (2008) 9710.
[23] D. Mores, E. Stavitski, M.H.F. Kox, J. Kornatowski, U. Olsbye, B.M. Weckhuysen, Chem. Eur. J. 14 (2008) 11320.
[24] Z.M. Cui, Q. Liu, Z. Ma, S.W. Bian, W.G. Song, J. Catal. 258 (2008) 83.
[25] D. Lesthaeghe, A. Horre, M. Waroquier, G.B. Marin, V. Van Speybroeck, Chem. Eur. J. 15 (2009) 10803.
[26] A. Bhan, E. Iglesia, Acc. Chem. Res. 41 (2008) 559.
[27] D. Lesthaeghe, B. De Sterck, V. Van Speybroeck, G.B. Marin, M. Waroquier, Angew. Chem. Int. Ed. 46 (2007) 1311.
[28] D. Lesthaeghe, V. Van Speybroeck, M. Waroquier, Phys. Chem. Chem. Phys. 11 (2009) 5222.
[29] B. Delley, J. Chem. Phys. 113 (2000) 7756.
[30] J.P. Perdew, K. Burke, M. Ernzerhof, Phys. Rev. Lett. 77 (1996) 3865.
[31] B. Delley, Phys. Rev. B 66 (2002) 155125.
[32] H.J. Monkhorst, J.D. Pack, Phys. Rev. B 13 (1976) 5188.
[33] A. Banerjee, N. Adams, J. Simons, R. Shepard, J. Phys. Chem. 89 (1985) 52.
[34] A.B. Bortz, M.H. Kalos, J.L. Lebowitz, J. Comput. Phys. 17 (1975) 10.
[35] S. Grimme, J. Comput. Chem. 27 (2006) 1787.
[36] S. Grimme, J. Comput. Chem. 25 (2004) 1463.
[37] C.M. Wang, Y.D. Wang, Z.K. Xie, Z.P. Liu, J. Phys. Chem. C 113 (2009) 4584.
[38] B.M. Lok, C.A. Messina, R.L. Patton, R.T. Gajek, T.R. Cannan, E.M. Flanigen, J. Am. Chem. Soc. 106 (1984) 6092.
[39] A.M. Vos, R.A. Schoonheydt, F. De Proft, P. Geerlings, J. Phys. Chem. B 107 (2003) 2001.
[40] B. Arstad, S. Kolboe, O. Swang, J. Phys. Chem. B 108 (2004) 2300.
[41] S. Kolboe, S. Svelle, B. Arstad, J. Phys. Chem. A 113 (2009) 917.
[42] O. Sekiguchi, V. Meyer, M.C. Letzel, D. Kuck, E. Uggerud, Eur. J. Mass Spectrom. 15 (2009) 167.
[43] F. Bleken, M. Bjorgen, L. Palumbo, S. Bordiga, S. Svelle, K.P. Lillerud, U. Olsbye, Top. Catal. 52 (2009) 218.
[44] S. Svelle, P.A. Ronning, S. Kolboe, J. Catal. 224 (2004) 115.
[45] S. Svelle, P.O. Ronning, U. Olsbye, S. Kolboe, J. Catal. 234 (2005) 385.
[46] S. Svelle, S. Kolboe, O. Swang, U. Olsbye, J. Phys. Chem. B 109 (2005) 12874.
[47] S. Svelle, C. Tuma, X. Rozanska, T. Kerber, J. Sauer, J. Am. Chem. Soc. 131 (2009) 816.